Hydrol. Earth Syst. Sci. Discuss., doi:10.5194/hess-2016-320, 2016
Manuscript under review for journal Hydrol. Earth Syst. Sci.
Published: 15 July 2016

Hydrology and Earth System Sciences
Discussions
Open Access

Effects of Multiple Doppler Radar data assimilation on the numerical simulation of a Flash Flood Event during the HyMeX campaign

Ida Maiello[1], Sabrina Gentile[1] , Rossella Ferretti[1,2], Luca Baldini[3], Nicoletta Roberto [3], Errico Picciotti[4,1], Pier Paolo Alberoni[5], Frank S. Marzano[6,1]

[1]CETEMPS, Department of Physical and Chemical Sciences - University of L'Aquila, L'Aquila, Italy

[2]Danish Meteorological Institute, Copenaghen, Denmark

[3]Institute of Atmospheric Sciences and Climate, CNR ISAC, Roma, Italy

[4]Himet s.r.l, L'Aquila, Italy

[5]Arpa Emilia Romagna - Servizio Idro-Meteo-Clima, Bologna, Italy

[6]Department of Electronic Engineering, Sapienza University of Rome, Rome, Italy

Correspondence to: Ida Maiello (ida.maiello@aquila.infn.it)

Abstract. An analysis to evaluate the impact of assimilating multiple radar data with a three dimensional variational (3D-Var) system on a heavy precipitation event is presented. The main goal is to establish a general methodology to quantitatively assess the performance of flash-flood numerical weather prediction at mesoscale. In this respect, during the first Special Observation Period (SOP1) of HyMeX (Hydrological cycle in the Mediterranean Experiment) campaign several Intensive Observing Periods (IOPs) were launched and nine occurred in Italy. Among them IOP4 is chosen for this study because of its low predictability. This event hit central Italy on 14 September 2012 producing heavy precipitation and causing several damages. Data taken from three C-band radars running operationally during the event are assimilated to improve high resolution initial conditions. In order to evaluate the impact of the assimilation procedure at different horizontal resolution and to assess the impact of assimilating multiple radars data, several experiments using Weather Research and Forecasting (WRF) model are performed. Finally, the statistical indexes as accuracy, equitable threat score, false alarm ratio and frequency bias are used to objectively compare the experiments, using rain gauges data as benchmark.

Keywords: *radar data assimilation, WRF, 3D-Var, HyMeX*

1 Introduction

The scientific community widely recognized the need of numerical weather prediction (NWP) models to run at high resolution for improving the very short term quantitative precipitation forecasts (QPF) during severe weather events and flash floods. The combination of NWP models and weather radar observations has shown improved skill with respect to extrapolation-based techniques (Sun et al., 2014). Nevertheless, the accuracy of the mesoscale NWP models is mostly subjected to the initial and lateral boundary conditions (IC and BC), and at the resolution of kilometers even more critical because of the lack of high resolution observations, beside for radar data. Several researches in the meteorological field have demonstrated that the assimilation of appropriate data into the NWP models, especially radar

(Sugimoto et al., 2009) and satellite data (Sokol 2009), significantly reduces the "spin-up" effect (Daley 1991) and improves the IC and BC of the mesoscale models. Classical observations such as TEMP (upper level temperature, humidity, and winds observations) or SYNOP (surface synoptic observations) have not enough density to describe for example local convection, while radar measurements can provide a sufficient density of data. Maiello et al. (2014) showed the positive effect of the assimilation of radar data into the precipitation forecast of a heavy rainfall event in central Italy. The authors showed the gain by using assimilating radar data with respect to the conventional ones. Similar results are obtained for a case of severe convective storm in Croatia by Stanesic and Brewster (2015).

Weather radar has a fundamental role in showing tridimensional structures of convective storms and the associated mesoscale and microscale systems (Nakatani, 2015). Xiao and Sun (2007) showed that, to better predict convective systems, radar observations into the NWP models at high resolution (2km) have to be assimilated. Recent researches in the meteorological area have established that the assimilation of real-time data, especially radar measurements (radial velocities and/or reflectivities), into the mesoscale NWP models can better predict precipitations for the next few hours (e.g. Xiao et al., 2005; Sokol and Rezacova, 2006; Dixon et al., 2009; Salonen et al., 2010).

The aim of this study is to investigate the potential of improving the NWP rainfall forecasts by assimilating multiple radars data. This may have a direct benefit also for hydrological applications, particularly for real time flash flood prediction. The novelty of the paper is in exploring impact on the high resolution forecast of the assimilation of multiple radars data in complex orography area such the Italian region to predict intense precipitation. This aim is reached by using the IOP4 of the SOP1 of the HyMeX campaign. The SOP1 was held from 5 September to 5 November 2012; the IOP4 was issued for the central Italy target area on 14 September 2012 and it was tagged both as a Heavy Precipitation Event (HPE) and a Flash Flood Event (FFE). Reflectivity from three C-band Doppler weather radars is ingested together with traditional meteorological observations (SYNOP and TEMP) using 3D-Var to improve WRF model performance.

The manuscript is arranged as follows. Section 2 provides information on the flash flood event and all the measurements to be ingested by WRF 3D-Var. Section 3 presents WRF model configuration and WRF 3D-Var data assimilation system. The results are showed and evaluated in the Fourth Section. Summary and conclusions are reflected in the last Section.

2 Study area and data

The HyMeX project (http://www.hymex.org) aims at a better understanding of the water cycle in the Mediterranean with focus on extreme weather events. The observation strategy of HyMeX is organized in a long-term (4 years) Enhanced Observation Periods (EOP) and short-term (2 months) Special Observation Periods (SOP). During the SOP1, that was held from 5 September to 5 November 2012, three Italian hydro-meteorological site were identified within the Western Mediterranean Target Area (TA): Liguria–Tuscany (LT), northeastern Italy (NEI) and central Italy (CI).

2.1 Case study

During IOP4 a deep trough entered the Tyrrhenian Sea slowly moving south eastward. Advection of cold air along the central Adriatic coast occurred producing instability over central and southern Italy, and enhanced the Bora flow over the northern Adriatic Sea. The heavy precipitations occurred in the morning of September 14 mainly along the central eastern Italian coast (Marche and Abruzzo regions), associated with the cut-off low over the Tyrrhenian Sea (Figure 1a, c). This structure lasted until 15th September (Figure 1b, d).

Figure 2 shows the interpolated map of 24h accumulated rainfall recorded from rain gauges network from September 14th to September 15th (00:00-00:00UTC) with a maximum accumulated rainfall on the highest peak of Abruzzo region approximately reaching 300mm in 24 hours. DEWETRA is an operational platform used by the Italian Civil Protection Department (DPC) and designed by CIMA Research Foundation to support operational activities at national or international scale. Rain gauges time series of some selected stations in Marche and Abruzzo regions where most of rainfall is accumulated during the event are presented in Figure 3: Fermo and Pintura di Bolognola (Marche region) respectively with nearly 130 mm/24h (Figure 3a) and 180 mm/24h (Figure 3b), Campo Imperatore, Atri and Pescara Colli (Abruzzo region) with respectively nearly 300mm/24h (Figure 3c), 160 mm/24h (Figure 3d) and 140 mm/24h (Figure 3e). It is clearly shown (Figure 3) that the incremental accumulation started around 02:00UTC of 14th September: in Fermo, Atri and Pescara Colli most of rainfall was concentrated in the first half of the day, whereas in Pintura di Bolognola and Campo Imperatore, precipitation fell all day long.

It is worthwhile to point out the large amount of hourly precipitation for Pescara and Atri respectively at 05:00UTC and 06:00UTC (red ovals in Fig. 3e and 3d respectively) reaching 45mm/h, indicating convective precipitation, whereas the precipitation on the Gran Sasso (Fig. 3c) was much weaker but lasting longer which allowed for reaching an accumulated amount of 300mm/24h.

Figure 4 reports a graphical tool that combines the Vertical Maximum Intensity (VMI) reflectivity from the Italian radar network (Vulpiani et al., 2008a) together with the Meteosat Second Generation (MSG) 10.8 µm image (in normalized inverted greyscale). VMI values above 45 dBZ are associated with intense precipitation occurred during convective events. Zoom over CI target area shows a line of convective cells along the Apennines in central Italy due to western flow approaching the orographic barrier.

2.2 Observations to be assimilated

Conventional observations SYNOP and TEMP were retrieved from the European Centre for Medium-Range Weather Forecasts (ECMWF) Meteorological Archival and Retrieval System (MARS). A total of 989 observations (967 SYNOP and 22 TEMP) are ingested into the coarse resolution domain, whereas a total of 338 (331 SYNOP and 7 TEMP) observations are ingested into the high resolution one.

Volumetric reflectivity taken from three C-band Doppler radars operational during the IOP4 have been assimilated to improve IC. Radars have different technical characteristics and were operated with different scanning strategies and operational settings. Data from the single polarization Doppler Mt. Midia radar (MM, 42°03'28'' N, 13°10'38''E, h=1760 m ASL, n°elevations=4, temporal resolution=15 min, range resolution=500 m) are provided by the Centro Funzionale of Abruzzo Region. The data from the dual polarization Doppler Polar 55C radar (POL, 41° 50' 24" N, 12° 38' 50"E, h=160.5 m ASL, n°elevations=6 or 8, temporal resolution=5 min, range resolution=75 m) are provided by ISAC-CNR of Rome; finally, data from the dual polarization Doppler San Pietro Capofiume radar (SPC, 44°23'24"N, 11°22'12"E, h=31 m ASL, n°elevations=6, temporal resolution=15 min, range resolution=250 m) are provided by Arpa Emilia Romagna. MM and SPC radars are included in the Italian radar network, while Polar 55C is a research radar working on demand which was operational during HyMeX IOPs (Roberto et al., 2016).

As is common knowledge, radar data can be affected by numerous sources of errors, mainly due to ground clutter, attenuation due to propagation or beam blocking, anomalous propagation and radio interferences. This is the reason why a preceding "cleaning" procedure is applied to the acquired radar reflectivity from the three radars before the assimilation method, consisting of the following 2 steps:

- pre-processing consists of a first quality check of radar volumes where radar pixel affected by ground clutter and anomalous propagation were filtered. Furthermore, Z was corrected for attenuation using a methodology based on the specific differential phase shift (K_{dp}) available for dual polarization radars (Vulpiani et al, 2015);
- conversion to the model format is applied to all radars data.

3 Methodology and sensitivity analysis design

The numerical weather prediction experiments are performed in this work using the non hydrostatic Advanced Research WRF (ARW) modeling system V3.4.1. It is a primitive equations mesoscale meteorological model, with terrain-following vertical coordinates and options for different physical parameterizations. Skamarock et al. (2008) provides a detailed overview of the model. WRF set up, advanced implementation and numerical investigations for flash flood forecast are described in this section.

3.1 WRF model set up

In this study, a configuration using two domains run independently is used: a 12km domain (263x185) that covers central Europe and west Mediterranean basin (referred as D01) is initialized using the ECMWF analyses at 0.25 degrees of horizontal resolution; an innermost domain, that covers the whole Italy (referred as D02), with a grid space of 3 km (445x449) using as BC and IC the output of the previous forecast at 12km. Both domains run with 37 unequally spaced vertical levels, from the surface up to 100 hPa (Figure 5).

Taking into account that the performance of a mesoscale model is highly related to the parameterization schemes, the main physics packages used in these experiments are set as for the operational configuration used at CETEMPS (Ferretti et al., 2014), which include (Skamarock et al., 2008): the “New” Thompson et al. 2004 microphysics scheme, the MYJ (Mellor-Yamada-Janjic) scheme for the PBL (planetary boundary layer), the Goddard shortwave radiation scheme and the RRTM (rapid radiative transfer model) longwave radiation scheme, the Eta similarity scheme for surface layer formulation and the Noah LSM (Land Surface Model) to parameterize physics of land surface. A few preliminary tests are performed to assess the best cumulus parameterization scheme to be used both for the coarse and finest resolution domain for this event. Hence the following parameterizations are tested: the new Kain–Fritsch and the Grell 3D schemes. The latter is an enhanced version of the Grell-Deveneyi scheme, in our simulations only used on the lowest resolution domain, when the option cugd_avedx (subsidence spreading) is switched on. Based on the results of these two cumulus parameterization schemes, the one producing the best precipitation forecast will be used to evaluate the impact of data assimilation.

3.2 3D-Var data assimilation method

Hydrol. Earth Syst. Sci. Discuss., doi:10.5194/hess-2016-320, 2016
Manuscript under review for journal Hydrol. Earth Syst. Sci.
Published: 15 July 2016

Data assimilation (DA) is the procedure by which observations are combined with the product (*first guess* or *background forecast*) of a NWP model and their corresponding error statistics to produce a bettered estimate (the *analysis*) of the true state of the atmosphere or ocean (Skamarock et al., 2008). The variational DA method realizes this through the iterative minimization of a penalty function (Ide et al., 1997):

$$J(\boldsymbol{x}) = J^b(\boldsymbol{x}) + J^0(\boldsymbol{x}) = \frac{1}{2}\{[\boldsymbol{y}^0 - H(\boldsymbol{x})]^T \boldsymbol{R}^{-1}[\boldsymbol{y}^0 - H(\boldsymbol{x})] + (\boldsymbol{x}-\boldsymbol{x}^b)^T \boldsymbol{B}^{-1}(\boldsymbol{x}-\boldsymbol{x}^b)\}, \quad (1)$$

where $\boldsymbol{x}^b$ is the first guess state vector, $\boldsymbol{y}^0$ is the assimilated observation vector, H is the observation operator that links the model variables to the observation variables and $\boldsymbol{x}$ is the unknown analysis state vector to be found by minimizing $J(\boldsymbol{x})$. Finally $\boldsymbol{B}$ and $\boldsymbol{R}$ are the background covariance error matrix and the observation covariance error matrix, respectively.

The minimization of the penalty function $J(\boldsymbol{x})$, displayed by Equation (1), is the a posteriori maximum likelihood estimate of the true atmosphere state, given the two fonts of a priori data that are $\boldsymbol{x}^b$ and $\boldsymbol{y}^0$ (Lorenc, 1986).

In this study the 3D-Var system developed by Barker et al. (2003, 2004) is used for assimilating radar reflectivity and conventional observations SYNOP and TEMP. The penalty function minimization is performed in a preconditioned control variable space, where the preconditioned control variables are pseudo relative humidity, stream function, unbalanced temperature, unbalanced potential velocity and unbalanced surface pressure. Because of radar reflectivity assimilation is considered, the total water mixing ratio q_t is chosen as the moisture control variable. The following Equation (2) presents the observation operator used by the 3D-Var to calculate reflectivity for the comparison with the observed one (Sun and Crook, 1997):

$$Z = 43.1 + 17.5\, log(\rho q_r), \quad (2)$$

where ρ and q_r are the air density in kg/m^3 and the rainwater mixing ratio in g/kg, respectively, while Z is the co-polar radar reflectivity factor expressed in dBZ. Since the total water mixing ratio q_t is used as the control variable, a warm rain process (Dudhia, 1989) is introduced into the WRF-3D-Var system: this allowed for producing the increments of moist variables linked to the hydrometeors.

The performance of the DA system widely depends on the goodness of the $\boldsymbol{B}$ matrix in Equation (1). In this study, a specific background error statistics is computed for both domains using the National Meteorological Center (NMC) method (Parrish and Derber, 1992). To evaluate the NMC-based error statistics, the differences between two forecasts at t+24 and t+12 (performed every day and valid at the same time), are used to calculate the domain-averaged error statistics for the entire SOP1 period (5 September - 5 November 2012).

3.3 Design of the numerical experiments

The simulations on the coarser resolution domain (D01) are run from 12:00UTC of 13 September 2012 and integrated for the following 96 hours, whereas runs on the finest resolution domain started at 00:00UTC of September 14 for a total of 48 hours of integration. The 00:00UTC coarser resolution WRF forecast is used as the first guess (FG) in the 3D-Var experiment that is the analysis time in the assimilation procedure. After assimilation, the lateral and lower boundary conditions are updated for the high resolution forecast. Finally, the new initial and boundary conditions are used for the model initialization (in a warm start regime) at 00:00UTC. As already pointed out a set of preliminary experiments are performed using different cumulus convective scheme to assess the best one to be used. The following experiments are performed without assimilation and using the convective scheme on the coarser resolution domain only: KAIN-FRITSCH (KF_MYJ); GRELL3D (GRELL3D_MYJ); GRELL3D associated to the CUGD factor (GRELL3D_MYJ_CUGD). A summary of these numerical experiments is given in Table 1.

The analysis of the results of these set of experiments allows establishing the best model configuration for the radar data assimilation experiments. The DA experiments aim to investigate:

1. the impact of the assimilation at low and high resolution by assimilating both conventional and non-conventional data at both resolutions;
2. the impact of the assimilation of different types of observations;
3. the impact of the different radars, which is investigated by performing experiment by assimilating conventional data and then adding radar one by one.

The following experiments are performed: i) the control simulation (CTL) without data assimilation; the assimilation of conventional data (SYNOP and TEMP) only (CON_LR_12KM); ii) the assimilation of radar data from MM only (CONMM_LR_12KM) are added; iii) the assimilation of POL radar is added to the previous experiments (CONMMPOL_LR_12KM); iv) the assimilation of the third radar data is added to the previous (CONMMPOLSPC_LR_12KM). Finally, an experiment to assess the role of the outer loop is performed (CONMMPOLSPC3OL_LR_12KM).

To include non-linearity into the observation operators and to evaluate the impact of data entering for each cycle, the multiple outer loops strategy is applied (Rizvi et al., 2008). According to this approach, the non-linear problem is solved iteratively as a progression of linear problems: the assimilation system is able to ingest more observations by running more than one analysis outer loop. The experiments are summarized in (Table 2).

The MET (Model Evaluation Tools) application (DTC, 2013), developed at the DTC (Developmental Testbed Center, NCAR), has been used to objectively evaluate the 12 hours accumulated precipitation produced by WRF on the high resolution domain. The observations used for the statistical evaluation were obtained from the Platform DEWETRA of the Department of Civil Protection and the comparison has been performed over central Italy target area using about 3000 rain gauges with a good cover throughout the area.

4 Results and discussion

In this section the results will be presented and discussed following the rationale of the previously introduced experiments and using statistical indexes for performance quantitative assessment.

4.1 Sensitivity test to cumulus parameterization

The 24h accumulated rainfall on central Italy simulated by the model both on D01 (left column) and D02 (right column) using a different cumulus parameterization scheme (Fig. 6, on line 1 Kain-Fritsch, on line 2 Grell 3D, on line 3 Grell 3D and cugd_avedx=3 activated) is shown. Comparing the model outputs (Fig. 6) and the rain gauge observations (Fig. 2), it is worth noting that best performance on D01 is obtained by Grell 3D which is able to simulate the peak precipitation cumulated in 24 hour (between 200 and 300 mm) over Gran Sasso (Fig. 6, lines 2 and 3), where as Kain-Fritsch (Fig. 6a) completely misses the peak of rainfall on Abruzzo region (red spot in Fig. 2). Moreover, the rainfall pattern is not properly reproduced.

Furthermore results suggest that the spreading of the convective downdraft over several grid points allows for improving the rainfall distribution at both resolution: both the main cells of heavy rainfall are correctly separated over Abruzzo both on D01 and D02 (Fig. 6e and 6f) and the rainfall pattern along the northeast coast of Abruzzo region is also reproduced (Fig. 6f). The statistical indices computed using MET are showed in the next figure. The MET statistical analysis support the previous finding: the GRELL3D_MYJ_CUDG (blue curve Fig. 7) in the range 5-30 mm/12h shows higher performances in terms of accuracy (ACC, Fig 7a), equitable threat score (ETS, Fig. 7b) and false alarm ratio (FAR, Fig. c) than the other two simulations. Also the frequency bias (FBIAS, Fig. 7d, green and blue curves) indicates the simulations performed with Grell 3D as the one producing better results. Indeed it shows values closer to1 (the best value) than Kain-Fritsch (red curve). Finally, the mean error (ME, Fig. 7e, blue curve) for Grell 3D with cugd_avedx activated has values close to 0 (perfect value).

Here after GRELL3D_MYJ_CUDG is referred as the control (CTL) experiment performed without any data assimilation. Therefore, a new set of simulations are performed following the previous strategies: data assimilation on low or high resolution domains or on both domains simultaneously; conventional data and/or radar data assimilation.

4.2 Impact of conventional and radar data assimilation on rainfall forecast: low versus high resolution

In figure 8 a preliminary comparison among the low resolution (12km) simulations is shown. The control simulation (CTL) without data assimilation is shown in Figure 8a; whereas the other panels show the experiments performed using the data assimilation.

Observing the outputs of different experiments (Fig. 8) listed in Table 2, best simulation is found for CONMMPOLSPC_LR_12KM (Fig.8e) for which an attempt to reproduce the rainfall maximum over Campo Imperatore (black arrow) is found: the rainfall amount is very well simulated, however a cell displacement is noticeable. Furthermore a quite good attempt to forecast precipitation along the coasts (black oval) is also found.

The statistical indices (Fig. 9) support this finding: the brown curve (CONMMPOLSPC_LR_12KM) is producing the best ACC and FAR for all thresholds, except for ETS where good values are found only for thresholds lower than 20 mm/12h.

Similarly to the above comparison, high resolution results are presented in figure 10 obtained performing data assimilation only on 12km domain (column 1), only on 3km (column 2) and both on 12km and 3km (column 3); to the top of figure 10 the CTL experiment on D02 is shown. Figure 10 is organized as follows: viewing panels by line, on line 1 all the simulations with conventional data assimilation (CON*) only are found; on line 2 all the experiments with the assimilation of the data from Mt. Midia radar added (CONMM*); on line 3 all the experiments with the assimilation of the data from 2 C-band radars added (CONMMPOL*); on line 4 all the experiments with the assimilation of the data from all 3 C-band radars added (CONMMPOLSPC*); on line 5 the simulations where the strategy of outer loop is adopted (CONMMPOLSPC3OL*). For these experiments the values of the main statistical indices (ACC, FBIAS, ETS, FAR) have been summarized over tables reporting only two thresholds of precipitation: 1 mm/12h and 20 mm/12h (light and heavy rain regimes).

Aiming to investigate the impact of the assimilation at different resolutions, we start analyzing figure 10 by column and comparing it with the observation (fig. 2); the statistical analysis is also used:

- column 1 (12KM): CTL produces an overestimation of the rainfall that is not corrected by the assimilation of conventional data, but assimilating the 3 radars and introducing the 3 outer loops (Fig. 10 column 1 line 4) the main cells are better reproduced. MET indices in Table 3 suggest that CTL and CONMMPOLSPC3OL_HR_12km are the simulations with the best response, secondly CONMM_HR_12KM;
- column 2 (3KM): a partial correction of the rainfall overestimation compared to column 1 is observed especially if all the radars are assimilated and the outer loop strategy is applied; the statistical indices in Table 4 show CONMMPOLSPC3OL_3KM as the best experiment among the assimilated ones;
- column 3 (12KM_3KM): rainfall overestimation was partially corrected compared to columns 1 and 2 by all experiments; the MET statistics in Table 5 shows that CTL and CONMMPOLSPC3OL_3KM_12KM are the experiments that return better values.

Summarizing, the previous analysis suggests that the frequency of rainfall overestimation for higher thresholds has been reduced by radar data assimilation performed only on D01. Furthermore, improvements come out for heavy rain regimes when radar data assimilation has been performed on the highest resolution domain, whereas the ingestion of conventional observations produces the worst results since a smaller number of them were assimilated into the finest resolution domain than that the coarser one. The assimilation, operated on both 12km and 3km, gives better results than the ones on column 1, but a response worse than the others on column 2 is given for higher thresholds.

In order to examine the impact of the assimilation of different data and radars, we can now analyze the experiments showed in figure 10 by line. The results are compared with the observations of Fig. 2. The following considerations are worth discussing:

- line 1 (CON): a strong reduction of the rainfall is found with respect to CTL if conventional data are assimilated, but the rainfall pattern remains unchanged; statistical indices in Table 6 seem do not improve performances of CTL. The indices values suggest a slightly better performance when the conventional observations are assimilated only on the bigger domain;
- line 2 (CONMM): a further reduction in the precipitation overestimation is found as well as some variations in the pattern of the rainfall; statistics in Table 7 shows that Mt. Midia radar data assimilation improves model performance above all for higher thresholds; conventional observations assimilation in tandem with MM gives better results;
- line 3 (CONMMPOL): a quite strong improvement in the rainfall amount is found for all simulations. From the statistics of Table 8 we have found a worsening of the results especially for heavy rain regimes when POL is added (FBIAS and ETS); a better answer is given by the simulation where assimilation is performed on both domains;
- line 4 (CONMMPOLSPC): a clear correction of the rainfall pattern is found; the overestimation produced by the simulation where all the radars are assimilated on the 3km domain has been corrected by the experiment in

which the radars are assimilated both on D01 and D02; statistical indices in Table 9 suggest that the addition of SPC radar improves the results, furthermore they are not better than those where only MM is ingested;

- line 5 (CONMMPOLSPC3OL): the outer loop experiment confirms the overestimation reduction by *12KM_3KM; from Table 10 it seems that the introduction of 3OL improves the indices values above all when the 12km domain is considered; CONMMPOLSPC3OL_12KM_3KM can be considered the best simulation.

In summary, simulations results show that assimilation of conventional observations is better to perform on the lowest resolution domain; with regard to the assimilation of radar data, due to its location Apennines range screen radar beam and POL underestimates rainfall where the peak precipitation occurs, passing to the model wrong estimates thus worsening assimilation results. Also the outer loop strategy could have an important role in the assimilation procedure, but this latter needs a further investigation because a general rainfall underestimation for higher thresholds is found.

5 Conclusions

The purpose of this manuscript has been to evaluate the effects of multiple radar data assimilation on a heavy precipitation event occurred during the SOP1 of the HyMeX campaign. A sensitivity study at different domain resolution and using different types of data to improve initial conditions has been performed by assimilating into the WRF model radar reflectivity measurements, collected by three C-band Doppler weather radars operational during the event that hit central Italy on 14 September 2012. The 3D-Var and MET are the WRF tools used to assess this purpose. First of all, WRF model responses to different type of cumulus parameterization have been tested to establish the best configuration and to obtain the control simulation. The latter has been compared with observations and other experiments performed using 3D-Var. The set of assimilation experiments have been conducted following two different strategies: i) data assimilation at low and high resolution or at both resolutions simultaneously; ii) conventional data against radar data assimilation. Both have been examined to assess the impact on rainfall forecast.

The major findings of this work have been the following:

- Grell 3D parameterization improves the simulations both on D01and D02 and the use of the spreading factor is an added value in properly predict heavy rainfall over inland of Abruzzo and the rainfall pattern along the northeast coast;
- investigating the impact of the assimilation at different resolutions, best results are showed by the experiments where the data assimilation is performed on both domains 12km and 3km;
- the impact of the assimilation using different types of observations shows improvements if all the radars together with conventional data are assimilated; furthermore MM is the one that better impact the model results because of it has been better detected the event;
- the outer loop strategy allows for further improving positive impact of the assimilation of multiple radars. Moreover, a deeper investigation of multiple outer loops strategy is required to assess its impact.

Analyzing the results obtained in this study, it is not possible to assess which is, in general, the best model configuration since this analysis should be performed systematically with a significant number of case studies. However, this work is providing a general approach that can encourage to investigate more flash flood cases in order to make the assimilation of multiple radars data suitable for operational use. In order to confirm and consolidate these initial findings, apart from analyzing more case studies, a "pseudo-operational" testing would be also useful.

Acknowledgements

We are grateful to the Gran Sasso National Laboratories for support in computing resources, as well as the National Civil Protection Department and CIMA Research Foundation for rain gauges data using for the model validation. NCAR is also acknowledge for WRF model and 3D-Var system. This work aims at contributing to the HyMeX programme.

References

Barker, D.M., Huang, W., Guo, Y.-G., and Bourgeois, A.: A Three-Dimensional Variational (3D-Var) Data Assimilation System For Use With MM5. NCAR Tech. Note, NCAR/TN-453+STR, UCAR Communications, Boulder, CO, 68pp, 2003.

Barker, D.M., Huang, W., Guo, Y.-R., Bourgeois, A., and Xiao, Q.: A Three-Dimensional Variational (3D-Var) Data Assimilation System For Use With MM5: Implementation and Initial Results. *Mon. Wea. Rev*., 132, 897-914, 2004.

Daley, R.: Atmospheric Data Analysis, Cambridge University Press, Cambridge, UK, 1991.

Developmental Testbed Center, 2013: MET: Version 4.1 Model Evaluation Tools Users Guide. Available at http://www.dtcenter.org/met/users/docs/overview.php. 226 pp.

Dixon, M., Li, Z., Lean, H., Roberts, N., and Ballard, S.: Impact of data assimilation on forecasting convection over the United Kingdom using a high-resolution version of the Met Office Unified Model, Mon. Weather Rev., 137, 1562–1584, 2009.

Dudhia, J.: Numerical study of convection observed during the winter monsoon experiment using a mesoscale two-dimensional model, J. Atmos. Sci., 46, 3077–3107, 1989.

Ferretti, R., E. Pichelli, S. Gentile, I. Maiello, D. Cimini, S. Davolio, M. M. Miglietta, G. Panegrossi, L. Baldini, F. Pasi, F. S. Marzano, A. Zinzi, S.Mariani, M. Casaioli, G. Bartolini, N. Loglisci, A. Montani, C. Marsigli,A.Manzato, A. Pucillo, M. E. Ferrario, V. Colaiuda, and R. Rotunno: Overview of the first HyMeX Special ObservationPeriod over Italy: observations and model results. Hydr. Earth Syst. Sci., 18, 1953-1977,2014, doi:10.5194/hess-18-1953-2014, 2014.

Ide, K., Courtier, P., Ghil, M., and Lorenc, A. C.: Unified notation for data assimilation: Operational, sequential and variational, J. Meteorol. Soc. Jpn., 75, 181–189, 1997.

Li Y., Wang X., and Xue M., 2008: Assimilation of radar radial velocity data with the WRF ensemble-3DVAR hybrid system for the prediction of hurricane Ike,*Mon. Wea Rev*, vol. 140, pp. 3507–3524.

Lorenc, A. C.: Analysis methods for numerical weather prediction, Q. J. Roy. Meteorol.Soc., 112, 1177–1194, 1986.

Maiello, I., Ferretti, R., Gentile, S., Montopoli, M., Picciotti, E., Marzano, F. S., and Faccani, C.: Impact of radar data assimilation for the simulation of a heavy rainfall case in central Italy using WRF–3DVAR, Atmos. Meas. Tech., 7, 2919-2935, doi:10.5194/amt-7-2919-2014, 2014.

Nakatani T., Misumi R., Shoji Y., Saito K., Seko H., Seino N., Suzuki S-I.,Shusse Y., Maesaka T., and Sugawara H. ; Tokyo metropolitan area convection study for extreme weather resilient cities. *BAMS*, 96, ES123-ES126, 2015.

Parrish, D.F. and Derber, J.C.: The National Meteorological Center's Spectral Statistical-Interpolation Analysis System. *Mon. Wea. Rev.*, 120, 1747-1763, 1992.

Rizvi, S., Guo, Y.-R, Shao, H., Demirtas, M., and Huang, X.-Y.: Impact of outer loop for WRF data assimilation system (WRFDA). 9th WRF Users' Workshop, Boulder, Colorado, 23-27 June 2008.

Roberto, N., Adirosi, E., Baldini, L., Casella, D., Dietrich, S., Gatlin, P., Panegrossi, G., Petracca, M., Sanò, P., and Tokay, A.: Multi-sensor analysis of convective activity in central Italy during the HyMeX SOP 1.1, Atmos. Meas. Tech., 9, 535-552, doi:10.5194/amt-9-535-2016, 2016.

Salonen K, Haase G, Eresmaa R, Hohti H, Järvinen H. 2010. Towards the operational use of Doppler Radar radial winds in HIRLAM. Atmospheric Research 100: 190–200.

Skamarock, W.C., Klemp, J.B., Dudhia, J., Gill, D.O., Barker, D.M., Duda, M. G., Huang, X.-Y., Wang, W., and Powers, J. G.: A description of the Advanced Reasearch WRF Version 3. NCAR Technical Note. TN 475+STR, 113 pp., available from www.mmm.ucar.edu/wrf/users/docs/arw_v3.pdf (last access: January 2012), 2008.

Sokol, Z. and Rezacova, D.: Assimilation of Radar reflectivity into the LMCOSMO model with a high horizontal resolution, Meteorol. Appl., 13, 317–330, 2006.

Sokol, Z.: Effects of an assimilation of Radar and satellite data on a very short range forecast of heavy convective rainfalls, Atmos. Res., 93, 188–206, 2009.

Stanesic A., and K.A. Brewester: Impact of Radar Data Assimilation on the Numerical Simulation of a Severe Storm in Croatia. Met.Zeit.DOI 10.1127/metz/2015/0574, 2015.

Sugimoto, S., Crook N.A., Sun J., Xiao Q., and Barker D.M., 2009: An examination of WRF 3D-VarRadar data assimilation on its capability in retrieving unobserved variables and forecasting precipitation through observing system simulation experiments. *Mon. Wea. Rev.*, 137, 4011-4029, DOI:10.1175/2009MWR2839.1.

Su, J. Xue, M., Wilson J. W., Zawadzki I., Ballard S.P., Onvlee-Hooimeyer J., Joe P., Barker D.M., Li P-W., Golding B., Xu M., and Pinto J.: Use of NWP for nowcasting convective precipitation, recent progress and challenges. *BAMS*, 95, 409-426, 2014.

Sun, J. and Crook, N.A.: Dynamical and Microphysical Retrieval from Doppler RADAR Observations Using a Cloud Model and Its Adjoint. Part I: Model Development and Simulated Data Experiments. *J. Atmos. Sci.*, 54, 1642-1661, 1997.

Thompson, G., R. M. Rasmussen, and K. Manning, 2004: Explicit forecasts of winter precipitation using an improved bulk microphysics scheme. Part I: Description and sensitivity analysis.

Mon. Wea. Rev.,132, 519–542.

Vulpiani G., Pagliara, P., Negri, M., Rossi, L., Gioia, A., Giordano, P., Alberoni, P. P., Cremonini, R., Ferraris, L., and Marzano, F. S.: The Italian radar network within the national early-warning system for multi-risks management, Proc. of Fifth European Conference on Radar in Meteorology and Hydrology (ERAD 2008), 184, Finnish Meteorological Institute, Helsinki, 30 June-4 July, 2008a.

Vulpiani, G., Baldini, L., and Roberto, N.: Characterization of Mediterranean hail-bearing storms using an operational polarimetric X-band radar, Atmos. Meas. Tech., 8, 4681-4698, doi:10.5194/amt-8-4681-2015, 2015.

Wang X., Barker D. M., Snyder C., and Hamill T. M., 2008: “A hybrid ETKF-3DVAR data assimilation scheme for the WRF model. Part I: observation system simulation experiment,” Monthly Weather Review, vol. 136, no. 12, pp. 5116–5131.

Xiao, Q., Kuo, Y.-H., Sun, J. and Lee, W.-C.: Assimilation of Doppler RADAR Observations with a Regional 3D-Var System: Impact of Doppler Velocities on Forecasts of a Heavy Rainfall Case. *J. Appl. Meteor.*,44, 768-788, 2005.

Xiao, Q. and Sun, J.: Multiple-RADAR Data Assimilation and Short-Range Quantitative Precipitation Forecasting of a Squall Line Observed during IHOP_2002. *Mon. Wea. Rev.*, 135, 3381-3404, 2007.

Hydrol. Earth Syst. Sci. Discuss., doi:10.5194/hess-2016-320, 2016
Manuscript under review for journal Hydrol. Earth Syst. Sci.
Published: 15 July 2016

Hydrology and Earth System Sciences
Open Access
Discussions

LIST OF FIGURES

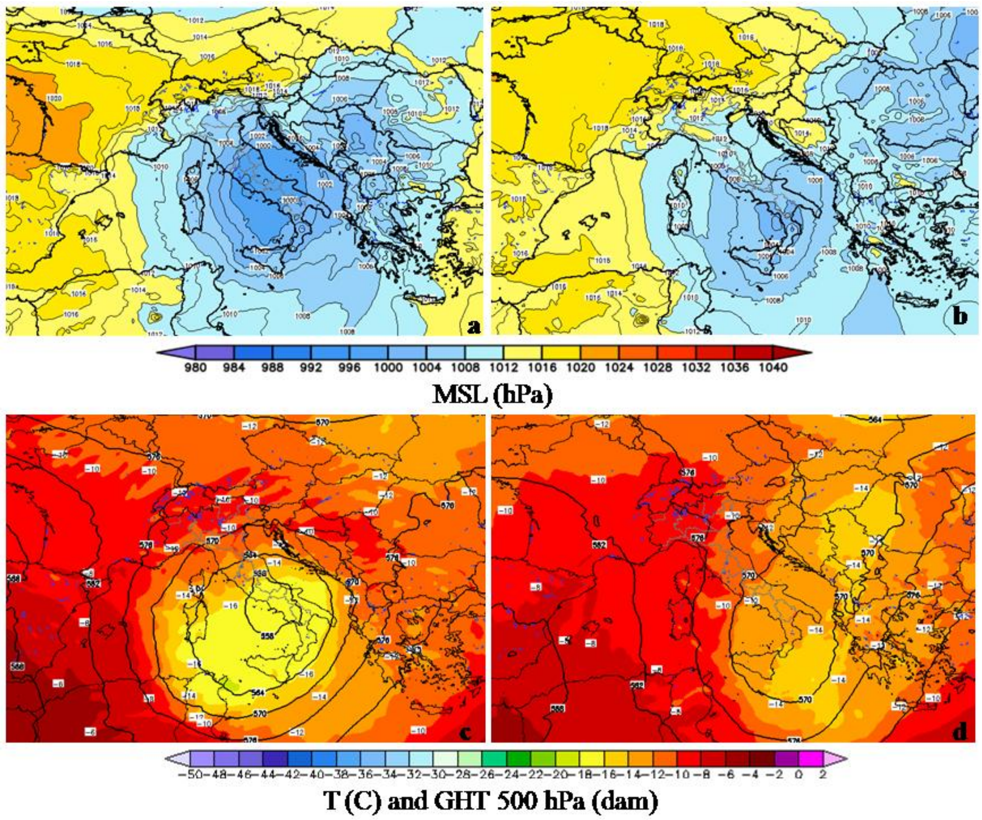

Figure 1: Mean sea level pressure (a, b), temperature and geopotential height at 500 hPa (c, d) at 12:00UTC on 14 September and 15September 2012, respectively.

Hydrol. Earth Syst. Sci. Discuss., doi:10.5194/hess-2016-320, 2016
Manuscript under review for journal Hydrol. Earth Syst. Sci.
Published: 15 July 2016

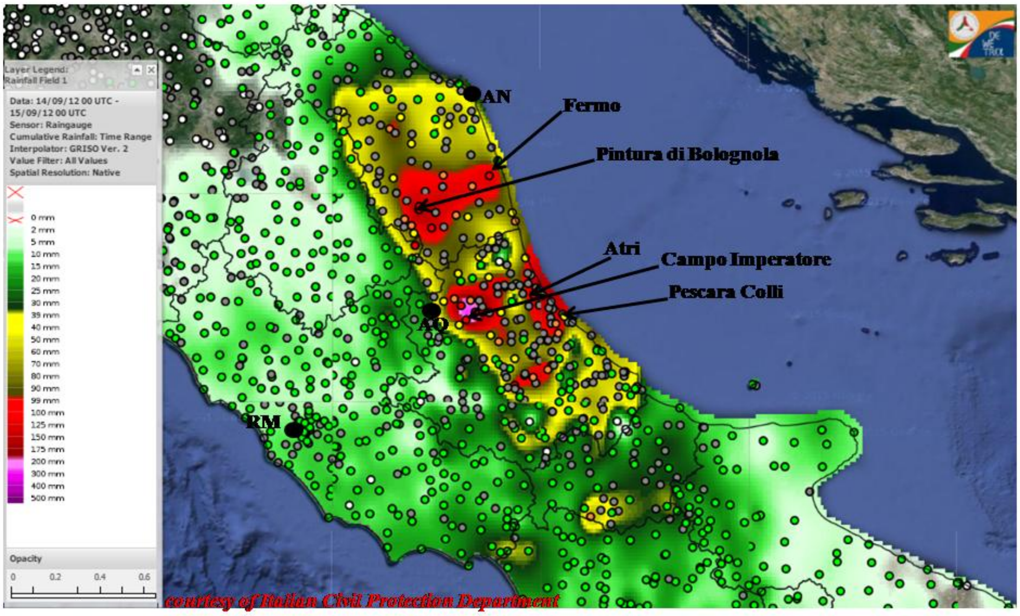

Figure 2: Interpolated map of 24h accumulated rainfall from 00:00UTC of 14 September 2012 over Abruzzo and Marche regions from DEWETRA system obtained by rain gauges measurements. Black contours are the administrative boundaries of Regions.

Hydrol. Earth Syst. Sci. Discuss., doi:10.5194/hess-2016-320, 2016
Manuscript under review for journal Hydrol. Earth Syst. Sci.
Published: 15 July 2016

Hydrology and Earth System Sciences
Open Access
Discussions

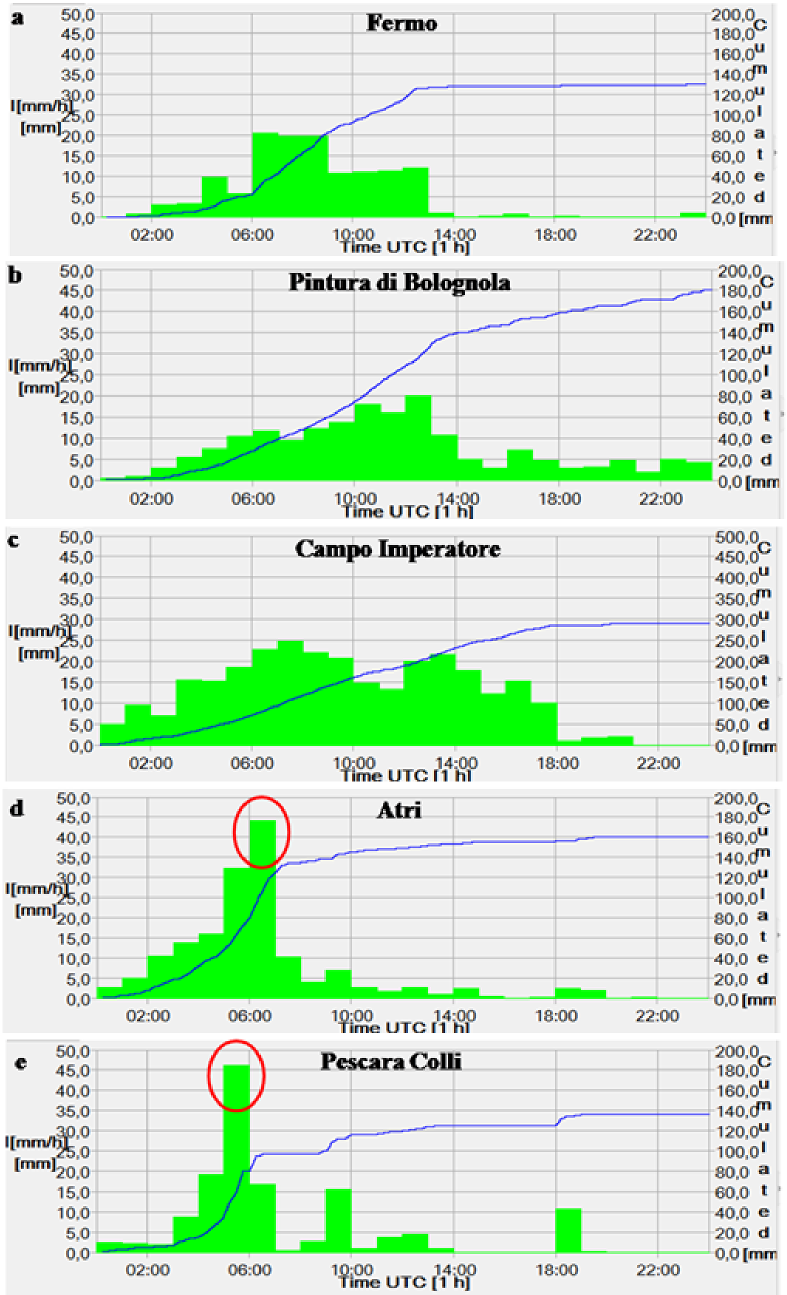

Figure 3: Rain gauges time series of some selected stations in Marche (a and b) and Abruzzo (c, d and e) regions during the event on 14 September 2012. The green histogram represents the hourly accumulated precipitation (scale on the left); the blue line represents incremental accumulation within the 24h (scale on the right). (*courtesy of Italian Civil Protection Department*)

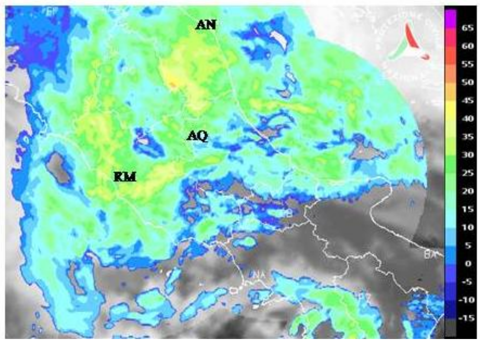

Figure 4: Zoom over CI of the VMI on 14September 2012 at 08:00UTC from the Italian radar network overlapped with the MSG (IR 10.8) at 07:30UTC. (*courtesy of Italian DPC*)

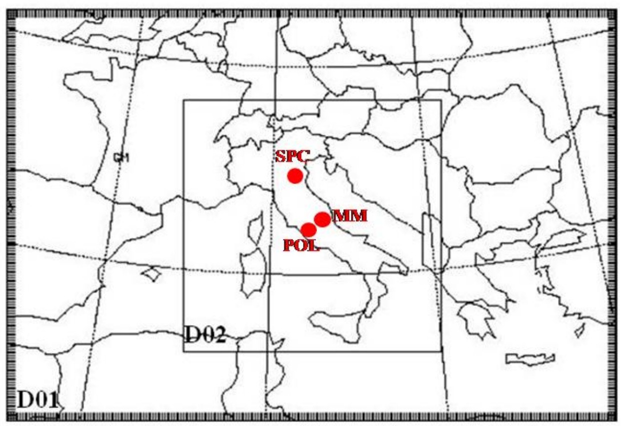

Figure 5: WRF nest-down domains configuration: the two domains have respectively resolution of 12 and 3 km. The high resolution D02 over Italy includes Mt. Midia (MM), ISAC-CNR (POL) and San Pietro Capofiume (SPC) radars (red dots in the figure).

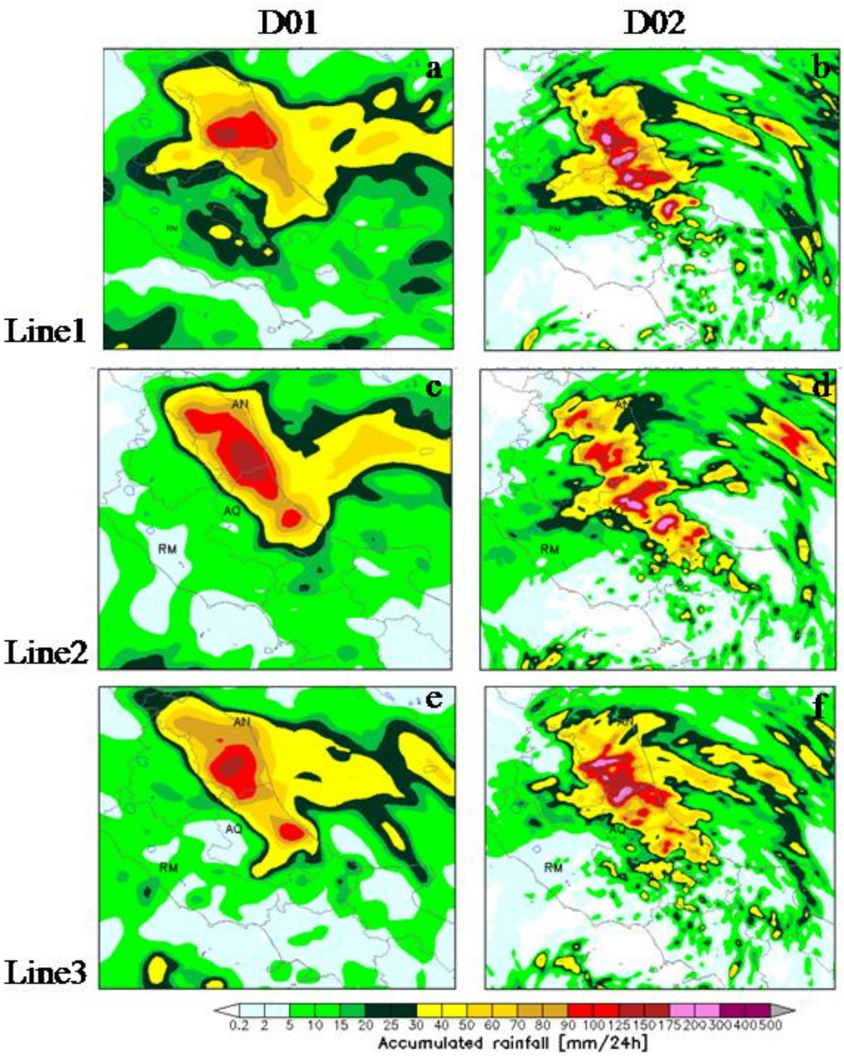

Figure 6: WRF accumulated 24h rainfall forecast on Central Italy from 00:00UTC of 14September 2012: a,b) D01 and D02 respectively run with Kain-Fritsch; c,d) D01 and D02 respectively run with Grell 3D; e,f) D01 and D02 respectively run with Grell 3D and cugd_avedx=3 activated.

Hydrol. Earth Syst. Sci. Discuss., doi:10.5194/hess-2016-320, 2016
Manuscript under review for journal Hydrol. Earth Syst. Sci.
Published: 15 July 2016

Hydrology and Earth System Sciences
Open Access
Discussions

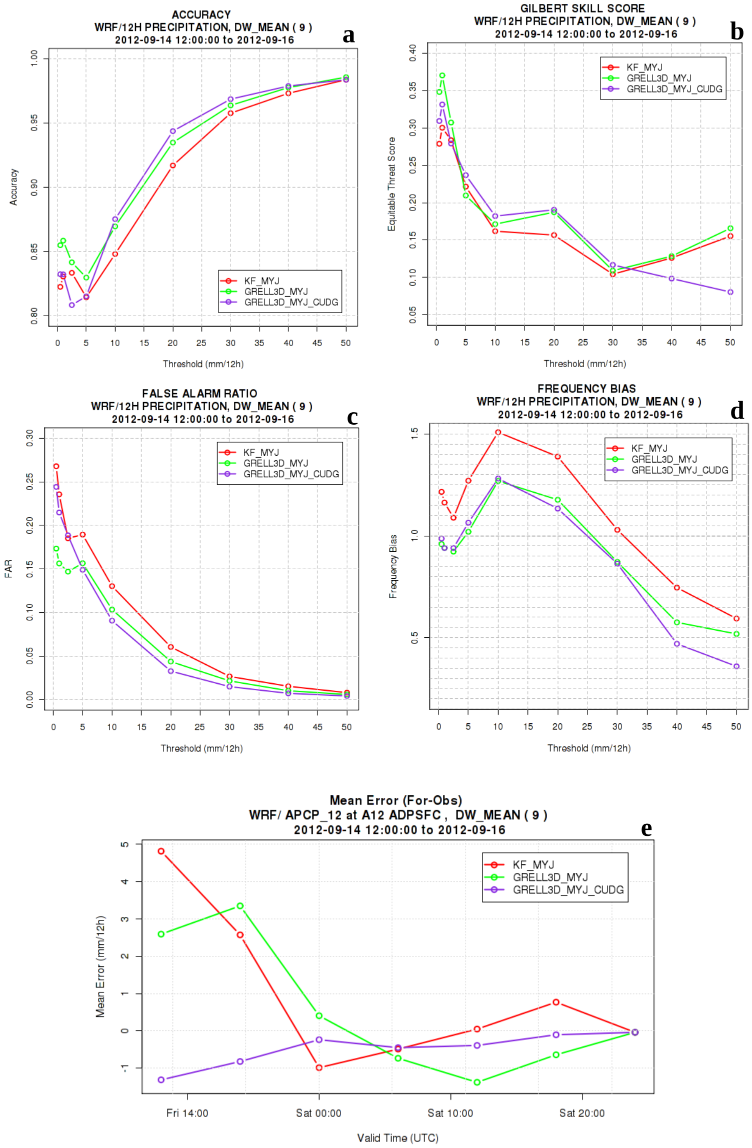

Figure 7: Forecast Accuracy (a), Equitable Threat Score (b), False Alarm Ratio (c), Frequency Bias (d) as a function of threshold and Mean Error (e) as a function of time. The red and green curves indicate Kain-Fritsch and Grell 3D simulations respectively, whereas the blue curve represents Grell 3D experiment with cugd_avedx=3 activated.

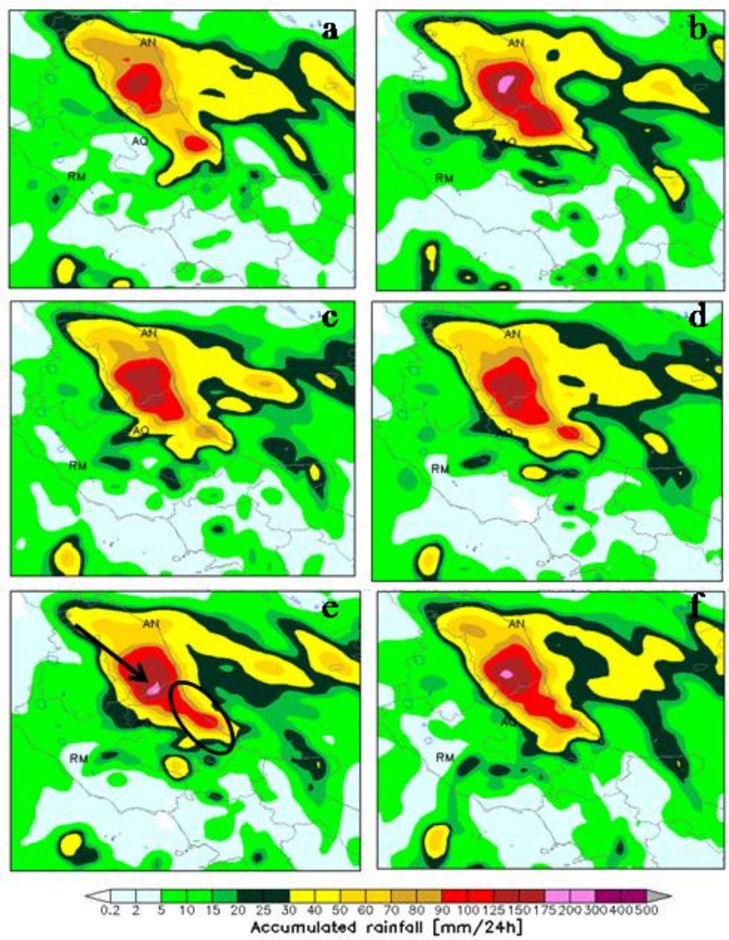

Figure 8: WRF D01 accumulated 24h rainfall forecast on Central Italy from 00:00UTC of 14 September 2012: a) WRF D01 CTL; b) WRF D01 CON_LR_12KM; c) WRF D01 CONMM_LR_12KM;d)WRF D01 CONMMPOL_LR_12KM; e) WRF D01 CONMMPOLSPC_LR_12KM; f) WRF D01 CONMMPOLSPC3OL_LR_12KM.

Hydrol. Earth Syst. Sci. Discuss., doi:10.5194/hess-2016-320, 2016
Manuscript under review for journal Hydrol. Earth Syst. Sci.
Published: 15 July 2016

Hydrology and Earth System Sciences
Open Access
Discussions

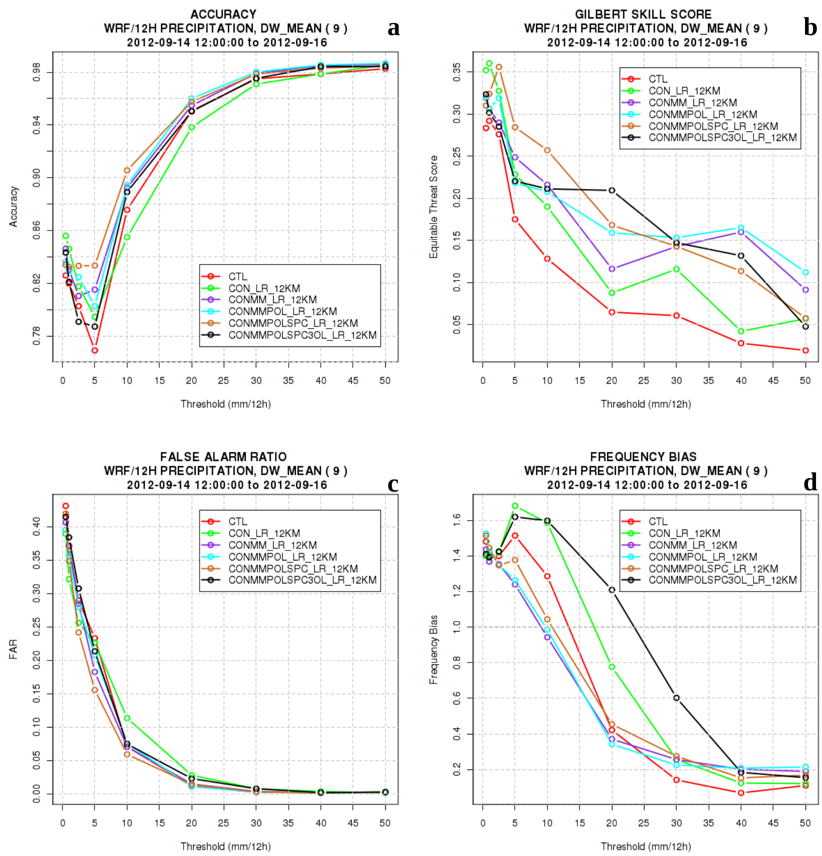

Figure 9: Forecast Accuracy (a), Equitable Threat Score (b), False Alarm Ratio (c) and Frequency Bias (d) as a function of threshold. The red curve indicates CTL experiment, the green curve CON_LR_12KM, the blue curve CONMM_LR_12KM, the cyan curve CONMMPOL_LR_12KM, the brown curve CONMMPOLSPC_LR_12KM, the black curve CONMMPOLSPC3OL_LR_12KM.

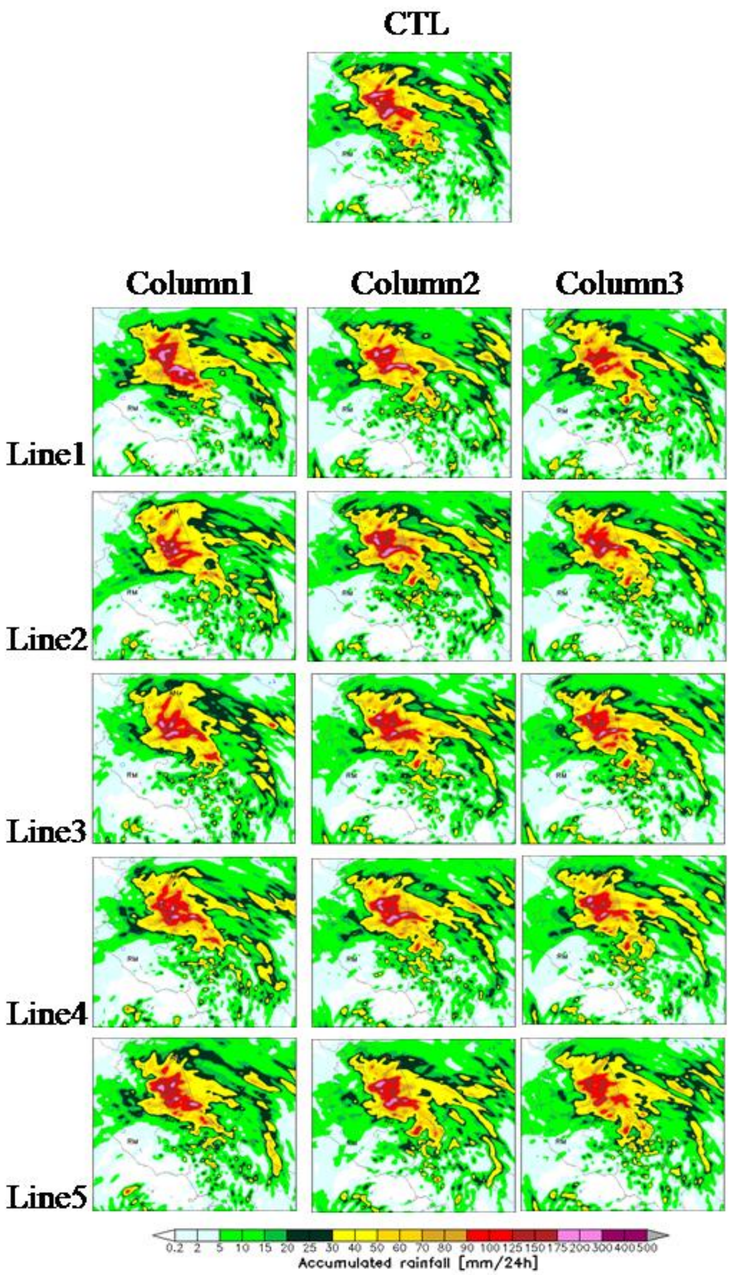

Figure 10: WRF D02 accumulated 24h rainfall forecast on Central Italy from 00:00UTC of 14 September 2012: CTL simulation (top center); on each column simulations obtained performing data assimilation at different resolutions (*12KM, *3KM, *12KM_3KM); on each line simulations performed assimilating different kinds of data (CON*, CONMM*, CONMMPOL*,CONMMPOLSPC*, CONMMPOLSPC3OL*).

Table 1: List of experiments to assess the cumulus parameterization.

Experiment	Cumulus	Grid Resolution	Assimilation Synop+Temp	Assimilation Radar
KF_MYJ	KAIN-FRITSCH	12KM/3KM	NO	NO
GRELL3D_MYJ	GRELL3D	12KM/3KM	NO	NO
GRELL3D_MYJ_CUGD (CTL)	GRELL3D+CUGD	12KM/3KM	NO	NO

Table 2: List of experiments to test the impact of data assimilation.

Experiment	Cumulus	Grid Resolution	Assimilation Synop+Temp	Assimilation Radar
CTL	GRELL3D+CUGD	12KM/3KM	NO	NO
CON	GRELL3D+CUGD	12KM/3KM/BOTH	YES	NO
CONMM	GRELL3D+CUGD	12KM/3KM/BOTH	YES	MM
CONMMPOL	GRELL3D+CUGD	12KM/3KM/BOTH	YES	MM+POL
CONMMPOLSPC	GRELL3D+CUGD	12KM/3KM/BOTH	YES	MM+POL+SPC
CONMMPOLSPC3OL	GRELL3D+CUGD	12KM/3KM/BOTH	YES	MM+POL+SPC with 3 outer loops

Hydrol. Earth Syst. Sci. Discuss., doi:10.5194/hess-2016-320, 2016
Manuscript under review for journal Hydrol. Earth Syst. Sci.
Published: 15 July 2016

Hydrology and Earth System Sciences
Open Access
Discussions

Table 3: Statistics referred to experiments in column 1: Forecast Accuracy (ACC), Frequency Bias (FBIAS), Equitable Threat Score (ETS), False Alarm Ratio (FAR) are considered as a function of thresholds (1mm/12h and 20mm/12h). The experiments are: CTL, CON_HR_12KM, CONMM_HR_12KM, CONMMPOL_HR_12KM, CONMMPOLSPC_HR_12KM, CONMMPOLSPC3OL_HR_12KM.

Experiment	**ACC** *Thresholds mm/12h*		**FBIAS** *Thresholds mm/12h*		**ETS** *Thresholds mm/12h*		**FAR** *Thresholds mm/12h*	
	1	*20*	*1*	*20*	*1*	*20*	*1*	*20*
CTL	0.83	0.94	0.94	1.13	0.33	0.19	0.21	0.03
CON_HR_12KM	0.81	0.93	0.91	1.12	0.25	0.17	0.26	0.04
CONMM_HR_12KM	0.82	0.94	0.95	0.99	0.28	0.17	0.24	0.03
CONMMPOL_HR_12KM	0.80	0.95	0.82	0.61	0.20	0.10	0.25	0.02
CONMMPOLSPC_HR_12KM	0.82	0.94	0.86	0.92	0.28	0.14	0.21	0.03
CONMMPOLSPC3OL_HR_12KM	0.82	0.95	0.93	0.84	0.30	0.16	0.20	0.03

Table 4: Statistics referred to experiments in column 2: Forecast Accuracy (ACC), Frequency Bias (FBIAS), Equitable Threat Score (ETS), False Alarm Ratio (FAR) are considered as a function of thresholds (1mm/12h and 20mm/12h). The experiments are: CTL, CON_3KM, CONMM_3KM, CONMMPOL_3KM, CONMMPOLSPC_3KM, CONMMPOLSPC3OL_3KM.

Experiment	**ACC** *Thresholds mm/12h*		**FBIAS** *Thresholds mm/12h*		**ETS** *Thresholds mm/12h*		**FAR** *Thresholds mm/12h*	
	1	*20*	*1*	*20*	*1*	*20*	*1*	*20*
CTL	0.83	0.94	0.94	1.13	0.33	0.19	0.21	0.03
CON_3KM	0.82	0.94	0.80	0.83	0.24	0.15	0.22	0.03
CONMM_3KM	0.82	0.94	0.96	0.96	0.26	0.17	0.24	0.03
CONMMPOL_3KM	0.81	0.95	0.94	0.84	0.23	0.11	0.24	0.03
CONMMPOLSPC_3KM	0.82	0.94	1.03	0.90	0.28	0.16	0.24	0.03
CONMMPOLSPC3OL_3KM	0.83	0.95	0.96	0.91	0.27	0.18	0.27	0.03

Table 5: Statistics referred to experiments in column 3: Forecast Accuracy (ACC), Frequency Bias (FBIAS), Equitable Threat Score (ETS), False Alarm Ratio (FAR) are considered as a function of thresholds (1mm/12h and 20mm/12h). The experiments are: CTL, CON_12KM_3KM, CONMM_12KM_3KM, CONMMPOL_12KM_3KM, CONMMPOLSPC_12KM_3KM, CONMMPOLSPC3OL_12KM_3KM.

Experiment	**ACC** *Thresholds mm/12h*		**FBIAS** *Thresholds mm/12h*		**ETS** *Thresholds mm/12h*		**FAR** *Thresholds mm/12h*	
	1	*20*	*1*	*20*	*1*	*20*	*1*	*20*
CTL	0.83	0.94	0.94	1.13	0.33	0.19	0.21	0.03

Hydrol. Earth Syst. Sci. Discuss., doi:10.5194/hess-2016-320, 2016
Manuscript under review for journal Hydrol. Earth Syst. Sci.
Published: 15 July 2016

Hydrology and Earth System Sciences
Discussions
Open Access
EGU

CON_12KM_3KM	0.81	0.95	0.84	0.73	0.20	0.14	0.27	0.02
CONMM_12KM_3KM	0.83	0.94	0.96	0.94	0.28	0.16	0.23	0.03
CONMMPOL_12KM_3KM	0.81	0.95	0.96	0.75	0.23	0.13	0.25	0.03
CONMMPOLSPC_12KM_3KM	0.81	0.95	1.04	0.79	0.26	0.17	0.28	0.02
CONMMPOLSPC3OL_12KM_3KM	0.83	0.95	0.98	0.73	0.30	0.18	0.25	0.02

Table 6: Statistics referred to experiments in line 1: Forecast Accuracy (ACC), Frequency Bias (FBIAS), Equitable Threat Score (ETS), False Alarm Ratio (FAR) are considered as a function of thresholds (1mm/12h and 20mm/12h). The experiments are: CTL, CON_3KM, CON_HR_12KM, CON_12KM_3KM.

Experiment	**ACC** *Thresholds mm/12h*		**FBIAS** *Thresholds mm/12h*		**ETS** *Thresholds mm/12h*		**FAR** *Thresholds mm/12h*	
	1	***20***	***1***	***20***	***1***	***20***	***1***	***20***
CTL	0.83	0.94	0.94	1.13	0.33	0.19	0.21	0.03
CON_3KM	0.82	0.94	0.80	0.83	0.24	0.15	0.22	0.03
CON_HR_12KM	0.81	0.93	0.91	1.12	0.25	0.17	0.26	0.04
CON_12KM_3KM	0.81	0.95	0.84	0.73	0.20	0.14	0.27	0.02

Table 7: Statistics referred to experiments in line 2: Forecast Accuracy (ACC), Frequency Bias (FBIAS), Equitable Threat Score (ETS), False Alarm Ratio (FAR) are considered as a function of thresholds (1mm/12h and 20mm/12h). The experiments are: CTL, CONMM_3KM, CONMM_HR_12KM, CONMM_12KM_3KM.

Experiment	**ACC** *Thresholds mm/12h*		**FBIAS** *Thresholds mm/12h*		**ETS** *Thresholds mm/12h*		**FAR** *Thresholds mm/12h*	
	1	***20***	***1***	***20***	***1***	***20***	***1***	***20***
CTL	0.83	0.94	0.94	1.13	0.33	0.19	0.21	0.03
CONMM_3KM	0.82	0.94	0.96	0.96	0.26	0.17	0.24	0.03
CONMM_HR_12KM	0.82	0.94	0.95	0.99	0.28	0.17	0.24	0.03
CONMM_12KM_3KM	0.83	0.94	0.96	0.94	0.28	0.16	0.23	0.03

Table 8: Statistics referred to experiments in line 3: Forecast Accuracy (ACC), Frequency Bias (FBIAS), Equitable Threat Score (ETS), False Alarm Ratio (FAR) are considered as a function of thresholds (1mm/12h and 20mm/12h). The experiments are: CTL, CONMMPOL_3KM, CONMMPOL_HR_12KM, CONMMPOL_12KM_3KM.

Experiment	**ACC** *Thresholds mm/12h*		**FBIAS** *Thresholds mm/12h*		**ETS** *Thresholds mm/12h*		**FAR** *Thresholds mm/12h*	
	1	***20***	***1***	***20***	***1***	***20***	***1***	***20***
CTL	0.83	0.94	0.94	1.13	0.33	0.19	0.21	0.03

Hydrol. Earth Syst. Sci. Discuss., doi:10.5194/hess-2016-320, 2016
Manuscript under review for journal Hydrol. Earth Syst. Sci.
Published: 15 July 2016

Hydrology and Earth System Sciences
Discussions
Open Access

CONMMPOL_3KM	0.81	0.95	0.94	0.84	0.23	0.11	0.24	0.03
CONMMPOL_HR_12KM	0.80	0.95	0.82	0.61	0.20	0.10	0.25	0.02
CONMMPOL_12KM_3KM	0.81	0.95	0.96	0.75	0.23	0.13	0.25	0.03

Table 9: Statistics referred to experiments in line4: Forecast Accuracy (ACC), Frequency Bias (FBIAS), Equitable Threat Score (ETS), False Alarm Ratio (FAR) are considered as a function of thresholds (1mm/12h and 20mm/12h). The experiments are: CTL, CONMMPOLSPC_3KM, CONMMPOLSPC_HR_12KM, CONMMPOLSPC_12KM_3KM.

Experiment	**ACC** ***Thresholds mm/12h***		**FBIAS** ***Thresholds mm/12h***		**ETS** ***Thresholds mm/12h***		**FAR** ***Thresholds mm/12h***	
	1	***20***	***1***	***20***	***1***	***20***	***1***	***20***
CTL	0.83	0.94	0.94	1.13	0.33	0.19	0.21	0.03
CONMMPOLSPC_3KM	0.82	0.94	1.03	0.90	0.28	0.16	0.25	0.03
CONMMPOLSPC_HR_12KM	0.82	0.94	0.86	0.92	0.28	0.14	0.21	0.03
CONMMPOLSPC_12KM_3KM	0.81	0.95	1.04	0.79	0.26	0.17	0.28	0.02

Table 10: Statistics referred to experiments in line 5: Forecast Accuracy (ACC), Frequency Bias (FBIAS), Equitable Threat Score (ETS), False Alarm Ratio (FAR) are considered as a function of thresholds (1mm/12h and 20mm/12h). The experiments are: CTL, CONMMPOLSPC3OL_3KM, CONMMPOLSPC3OL_HR_12KM, CONMMPOLSPC3OL_12KM_3KM.

Experiment	**ACC** ***Thresholds mm/12h***		**FBIAS** ***Thresholds mm/12h***		**ETS** ***Thresholds mm/12h***		**FAR** ***Thresholds mm/12h***	
	1	***20***	***1***	***20***	***1***	***20***	***1***	***20***
CTL	0.83	0.94	0.94	1.13	0.33	0.19	0.21	0.03
CONMMPOLSPC3OL_3KM	0.83	0.95	0.96	0.91	0.27	0.18	0.27	0.03
CONMMPOLSPC3OL_HR_12KM	0.82	0.95	0.93	0.84	0.30	0.16	0.20	0.03
CONMMPOLSPC3OL_12KM_3KM	0.83	0.95	0.98	0.73	0.30	0.18	0.25	0.02